Available online at www.sciencedirect.com

SCIENCE DIRECT®

Thermochimica Acta 429 (2005) 189–203

thermochimica acta

www.elsevier.com/locate/tca

Enthalpy of dilution of $[SO_2 + salt + H_2O]$ in $[salt + H_2O]$ $\{salt = (NH_4)_2SO_4$ or $Na_2SO_4\}$: Experimental results and modeling

Álvaro Pérez-Salado Kamps, Viktor Ermatchkov, Eckehard Meyer, Gerd Maurer*

Chair of Applied Thermodynamics, University of Kaiserslautern, P.O. Box 30 49, D-67653 Kaiserslautern, Germany

Received 7 January 2005; received in revised form 1 March 2005; accepted 7 March 2005
Available online 19 April 2005

Abstract

New experimental results are presented for the enthalpy change upon diluting aqueous solutions of sulfur dioxide containing a salt (either ammonium sulfate or sodium sulfate) in aqueous solutions of that salt at about 313 and 352 K. A previously developed thermodynamic model for the vapor–liquid equilibrium of the chemical reacting systems $\{SO_2 + (NH_4)_2SO_4 + H_2O\}$ and $(SO_2 + Na_2SO_4 + H_2O)$ is extended allowing for the formation of pyrosulfite and for the description of the new experimental results for the enthalpy change upon dilution.

Keywords: Enthalpy of dilution; Sulfur dioxide; Ammonium sulfate; Sodium sulfate; Chemical reacting aqueous solutions

1. Introduction

Aqueous solutions of weak electrolyte gases (like ammonia, sulfur dioxide, hydrogen sulfide, carbon dioxide, etc.) and strong electrolytes {for example, inorganic salts such as (ammonium or sodium) (chloride or sulfate)} have to be treated in many processes related to the chemical, power and oil industries (e.g., in coal gasification, in wet flue gas desulfurization, or in water washing processes of catalytic cracker overhead systems). Both the energy costs and the restrictions imposed by environmental jurisdiction are continuously growing. In order to design and optimize those processes to meet these requirements and still run profitably, there is a demand for reliable models for the thermodynamic properties of such complex, chemical reacting mixtures. The basic design of the separation equipment requires experimental information on the equilibrium properties (i.e., basically vapor–liquid equilibrium data and information on the energy to vaporize/condense the mixtures) as well as on the kinetics of the chemical reactions and of the mass transfer processes.

The equilibrium speciation of the liquid mixtures must be known reliably in order to enable a description of the equilibrium properties. This does also hold for the kinetic processes, as the driving force for any kinetic process results from the deviation from equilibrium. Experimental information on the speciation might be obtained by spectroscopic investigations (cf., e.g., Ermatchkov et al. [1], Lichtfers and Rumpf [2], and Lichtfers [3]). Although such (often expensive) experiments may sometimes result only in qualitative information, they help to identify the important species. In many cases, model predictions for the speciation may considerably be improved by additionally taking into account experimental information on the enthalpy change upon dilution of those chemical reacting systems. This enthalpy change results primarily from (several) chemical reactions, but also from the change in the physical interactions resulting from the dilution.

In previous work, a thermodynamic model describing the vapor–liquid equilibrium of the chemical reacting systems $\{SO_2 + (NH_4)_2SO_4 + H_2O\}$ and $(SO_2 + Na_2SO_4 + H_2O)$ was developed (Rumpf and Maurer [4]). The model was mainly based on experimental results for the vapor–liquid equilibrium of the systems $(SO_2 + H_2O)$, $\{(NH_4)_2SO_4 + H_2O\}$, $(Na_2SO_4 + H_2O)$, $(H_2SO_4 + H_2O)$, $\{SO_2 + (NH_4)_2SO_4 + H_2O\}$, $(SO_2 + Na_2SO_4 + H_2O)$, and

---

* Corresponding author. Tel.: +49 631 205 2410; fax: +49 631 205 3835.
E-mail address: gmaurer@rhrk.uni-kl.de (G. Maurer).

0040-6031/$ – see front matter © 2004 Elsevier B.V. All rights reserved.
doi:10.1016/j.tca.2005.03.005

Nomenclature

a_i	activity of species i (on the molality scale)
A_B	effective cross sectional area of the diaphragm bellows
B	effective second osmotic virial coefficient in Pitzer's G^E equation for interactions between gas G and salt MX
C^ϕ	effective third osmotic virial coefficient in Pitzer's G^E equation for interactions between M and X
$f(I)$	Pitzer's modification of the Debye-Hückel term
$g(x)$	cf. Eq. (10)
G^E	Gibbs excess energy (on the molality scale)
h_i	(partial) molar enthalpy of species i
I	ionic strength (on the molality scale)
k_B	elastic force constant of the diaphragm bellows
$k_{H,i}$	Henry's constant of gas i in water (on the molality scale)
K_r	equilibrium constant for chemical reaction r (on the molality scale)
m_i	true molality of species i
m°	reference molality ($m^\circ = 1\ \mathrm{mol\ kg^{-1}}$)
$\bar{m}_i$	stoichiometric molality of component i
$\tilde{m}$	mass
M	cation
M_W^*	molar mass of water divided by $1000\ \mathrm{g\ mol^{-1}}$ ($M_W^* = 0.01801528$)
n_i	true amounts-of-substance of species i
$\bar{n}_i$	stoichiometric amounts-of-substance of component i
p	pressure
p_W^s	vapor pressure of pure water
Q_{diss}	energy (heat) involved in the movement of the punching knife
Q_{dil}	(experimental) heat of dilution
R	universal gas constant
T	absolute temperature
$v_i^{(\infty)}$	partial molar volume of gas i infinitely diluted in water
v_W	molar volume of water
V	volume
W_{diss}	energy (work) involved in the movement of the punching knife
X	anion
y_i	vapor phase mole fraction of component i
Y	anion
z_i	number of charges on the solute i

Greek Letters

$\alpha_{ij}^{(k)}$	binary parameter in Pitzer's G^E equation ($k = 1, 2$)
$\beta_{ij}^{(k)}$	parameters in Pitzer's G^E equation ($k = 0, 1, 2$) describing binary interactions (between solutes i and j in water)
γ_i	activity coefficient of species i (on the molality scale)
Γ	effective third osmotic virial coefficient in Pitzer's G^E equation for interactions between gas G and salt MX
$\Delta_{dil}H$	enthalpy change upon dilution
$\Delta_r h^{(ref)}$	$=\Delta_r H$ (see Eq. (23))
$\Delta_r H$	(molar) reaction enthalpy of reaction r (on the molality scale)
Δz	experimental uncertainty in property z
$\Delta \xi_r$	difference in extent of reaction r before and after mixing (Eq. (18))
λ_{ij}	second osmotic virial coefficient in Pitzer's G^E equation
μ_{ijk}	third osmotic virial coefficient in Pitzer's G^E equation = parameter describing ternary interactions (between solutes i, j, and k in water)
$\nu_{i,r}$	stoichiometric factor of reactant i in reaction r ($\nu_{i,r} > 0$ for a product and $\nu_{i,r} < 0$ for an educt)
ν_+, ν_-	number of cations and anions in electrolyte MX
ξ_r	extent of reaction r
ρ	specific density of the aqueous solutions
ϕ_i	vapor phase fugacity coefficient of component i

Superscripts

(exp)	experimental
(corr)	correlation
E	excess quantity
(l)	lower chamber
(pred)	prediction
(ref)	reference state (based on the molality scale)
s	saturation
(u)	upper chamber
(2)	after mixing

Subscripts

diss	dissipation
dil	dilution (of a solution)
G	gas G
r	reaction r
s	salt
W	water

($SO_2 + H_2SO_4 + H_2O$) and covered a temperature range from about 313–393 K. It took into account four sulfur containing ionic species in the aqueous phase: sulfate, bisulfate, sulfite, and bisulfite.

In the present work, the heat accompanying the (isothermal) dilution of liquid $\{SO_2 + (NH_4)_2SO_4 + H_2O\}$ by liquid

$\{(NH_4)_2SO_4 + H_2O\}$ and of liquid $(SO_2 + Na_2SO_4 + H_2O)$ by liquid $(Na_2SO_4 + H_2O)$ is determined at $T \approx 313$ and 352 K. The previous model is revised allowing for the description of these new calorimetric experimental results as well as for the description of experimental results from calorimetric investigations (enthalpy change upon dilution in pure water) of $(SO_2 + H_2O)$, $\{(NH_4)_2SO_4 + H_2O\}$, $(Na_2SO_4 + H_2O)$, and $(H_2SO_4 + H_2O)$ taken from the literature.

We recently presented experimental results from attenuated total reflectance (ATR)-IR spectroscopy of liquid mixtures of $(SO_2 + NH_3 + H_2O)$ revealing that pyrosulfite is an important sulfur-containing species in such aqueous solutions (Ermatchkov et al. [1]). Therefore, a previously developed thermodynamic model describing the vapor–liquid equilibrium of the chemical reacting system $(SO_2 + NH_3 + H_2O)$ was recently extended in order to account for the presence of pyrosulfite. In addition, new experimental results on the enthalpy change upon dilution of $(SO_2 + NH_3 + H_2O)$ in pure water was taken into account in the process of parameterization of that extended model (cf. Pérez-Salado Kamps et al. [5]). Although preliminary model calculations revealed that pyrosulfite may not appear in high concentrations in the aqueous solutions investigated in the present work $[\{SO_2 + (NH_4)_2SO_4 + H_2O\}$, and $(SO_2 + Na_2SO_4 + H_2O)]$, the formation of pyrosulfite is taken into account by the new thermodynamic model when the vapor–liquid equilibrium and the enthalpy change upon dilution of those systems is described, in order to enable a consistent transition to quaternary systems, such as for example $\{NH_3 + SO_2 + (NH_4)_2SO_4 + H_2O\}$ and $\{NH_3 + SO_2 + Na_2SO_4 + H_2O\}$, which will be investigated in a forthcoming publication.

2. Experimental

2.1. Apparatus

The batch calorimeter and the experimental arrangement used are both basically the same as in previous investigations [1,5–8]. Therefore, only a short description is given here. In an experiment, two identical pressurized mixing cells were placed into a Calvet-type batch calorimeter (MS 70, SETARAM, Lyon, France). One cell was used as reference in a differential arrangement, the other for the actual experiment. Each cell consists of an upper and a lower chamber separated by a thin Teflon foil. The lower chamber was filled with the aqueous salt solution [either $\{(NH_4)_2SO_4 + H_2O\}$ or $(Na_2SO_4 + H_2O)]$ with a syringe. The upper chamber was evacuated and filled with the aqueous gas containing solution [either $\{SO_2 + (NH_4)_2SO_4 + H_2O\}$ or $(SO_2 + Na_2SO_4 + H_2O)]$. The composition of those solutions were known from preparation. The stoichiometric molality of the salt was equal in both chambers, in order to avoid salt dilution effects. The amounts of mass of water + salt (in the lower chamber) and water + salt + gas (in the upper chamber) were determined by weighing the cell before and after the filling procedures. The cells were pressurized (using nitrogen from a storage tank) via a diaphragm bellows connected to the upper chamber. This arrangement avoided the (partial) evaporation of the liquid. The temperature in the batch calorimeter was determined with calibrated platinum resistance thermometers (with an uncertainty better than ±0.1 K). After thermal equilibration in the batch calorimeter the Teflon foil separating both compartments in a cell was cut by a punching knife (which is mounted inside the cell so that it can be moved from the outside) and the solutions were mixed. During mixing, the diaphragm bellows compensated for pressure changes resulting from the density change inside the cell. The calorimeter response was determined and converted to the heat of dilution Q_{dil} (using calibration curves, cf. Weyrich [8] and Hasse and Maurer [9]). The maximum uncertainty of that measured heat (±2%) was estimated from the calibration experiments.

In a typical experiment about 30 g of the gas containing aqueous salt solution were diluted with about 18 g of the gas free aqueous salt solution. The masses of the solutions were determined by weighing with a maximum uncertainty of ±0.008 g. At a fixed temperature, for each concentration of (SO_2 and salt), at least two (but up to 10) experiments with almost identical masses in the upper and lower chamber of the mixing cell were performed.

2.2. Substances

Sulfur dioxide (≥99.98 mol %) was purchased from Messer-Griesheim (Ludwigshafen, Germany). It was used without further purification. Deionized water was degassed by vacuum distillation. Sodium sulfate (≥99 mass%) and ammonium sulfate (≥99.5 mass%) were purchased from Merck GmbH (Darmstadt, Germany). The salts were degassed and dried under vacuum for several hours.

The salt-containing solutions were prepared in a storage tank. The stoichiometric molality of the salt in the aqueous solution was determined gravimetrically with a relative uncertainty smaller than 0.15%. The aqueous gas containing salt solutions were prepared as previously described in detail [6]: An evacuated cylinder sealed with a piston was partially filled with the aqueous salt solution. Known amounts of sulfur dioxide were added to the lower compartment of the cylinder from a storage tank. The mixture was pressurized by applying a rather high pressure on the upper side of the piston to avoid vaporization. The relative uncertainty in the stoichiometric molality of sulfur dioxide is smaller than 0.5%.

3. Experimental results

The enthalpy change $\Delta_{dil}H$ upon dilution of aqueous solutions of {sulfur dioxide + (ammonium sulfate or sodium sulfate)} in aqueous solutions of (ammonium sulfate or sodium sulfate, respectively) was calculated from the measured heat of dilution Q_{dil} applying corrections for (a) the work involved in the movement of the punching knife ($W_{\text{diss}} = -Q_{\text{diss}}$, which ranged from about 0.2–1 J and was determined in blind experiments), and (b) for the work accompanied by the change of the volume (V) of the liquids upon mixing, which was estimated by assuming an isothermal volume change upon mixing, which, as the diaphragm bellows is elastic, also causes a (small) change in the pressure (p) [1,6,8]:

$$\Delta_{\text{dil}} H \approx Q_{\text{dil}} + W_{\text{diss}} + \int V \mathrm{d}p \tag{1}$$

The last contribution was calculated from the density (ρ) of the solutions (which is estimated from a few measurements with a vibrating tube densimeter) and the elastic force constant ($k_B = 41.1$ N/cm) and effective cross sectional area ($A_B = 1.96\,\text{cm}^2$) of the diaphragm bellows (cf. refs. [6,8]):

$$\int V \mathrm{d}p = \frac{k_B}{2A_B^2}\left[\left(\frac{\tilde{m}^{(u)} + \tilde{m}^{(l)}}{\rho^{(2)}}\right)^2 - \left(\frac{\tilde{m}^{(u)}}{\rho^{(u)}} + \frac{\tilde{m}^{(l)}}{\rho^{(l)}}\right)^2\right] \tag{2}$$

3.1. System $\{SO_2 + (NH_4)_2SO_4 + H_2O\}$

The experimental results (at about 312.7 and 351.6 K) are given in Table 1. The enthalpy change upon dilution of aqueous solutions of $\{SO_2 + (NH_4)_2SO_4\}$ in aqueous solutions of $(NH_4)_2SO_4$ with equal stoichiometric salt molalities in the upper and lower chamber, $\bar{m}_s^{(u)} = \bar{m}_s^{(l)} \approx (1 \text{ and } 3.9)\,\text{mol kg}^{-1}$, is plotted versus the stoichiometric molality of the gas (in the upper chamber, $\bar{m}_{SO_2}^{(u)}$) in Fig. 1 ($T = 312.7$ K in the left diagram, $T = 351.6$ K in the right diagram). Fig. 1 additionally shows the experimental results for the enthalpy change upon dilution of aqueous solutions of SO_2 in pure water reported previously [5]. When there is no salt, exothermic behavior is observed. Adding small amounts of ammonium sulfate results in smaller absolute enthalpy changes, i.e., a shift towards endothermic behavior is observed. The experimentally determined numbers for the enthalpy change range from about −40 to 14 J. The correction term resulting from $\int V \mathrm{d}p$ ranges from about −1.5 to 1.2 J.

3.2. System $(SO_2 + Na_2SO_4 + H_2O)$

The experimental results (at about 312.7 and 351.7 K) are given in Table 2. The enthalpy change upon dilution of aqueous solutions of $\{SO_2 + Na_2SO_4\}$ in aqueous solutions of Na_2SO_4 with equal stoichiometric salt molalities in the upper and lower chamber, $\bar{m}_s^{(u)} = \bar{m}_s^{(l)} \approx (1 \text{ and } 1.2)$ and $(1 \text{ and } 1.45)\,\text{mol kg}^{-1}$ at 312.7 and 351.7 K, respectively, is plotted versus the stoichiometric molality of the gas (in the upper chamber, $\bar{m}_{SO_2}^{(u)}$) in Fig. 2 ($T = 312.7$ K in the left diagram, $T = 351.7$ K in the right diagram). Fig. 2 also shows the experimental results (from ref. [5]) for the enthalpy change upon dilution of aqueous solutions of SO_2 in pure water. As already mentioned, when there is no salt,

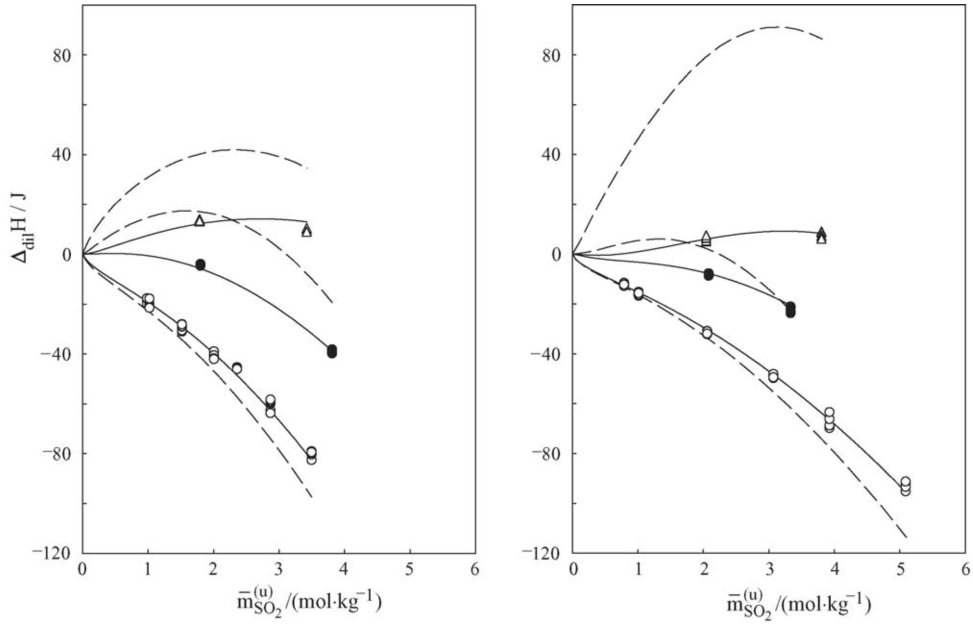

Fig. 1. Enthalpy change upon dilution of about 29.7 g $\{SO_2 + (NH_4)_2SO_4 + H_2O\}$ with about 18.2 g $\{(NH_4)_2SO_4 + H_2O\}$ at equal stoichiometric salt molality $\bar{m}_{(NH_4)_2SO_4}$ in the upper and lower chamber, plotted against the stoichiometric molality of the gas in the upper chamber ($\bar{m}_{SO_2}^{(u)}$) ($T = 312.7$ K in the left diagram, $T = 351.6$ K in the right diagram). Experimental results: (○)$\bar{m}_{(NH_4)_2SO_4} = 0$ (from ref. [5]), (●,△)$\bar{m}_{(NH_4)_2SO_4} \approx 1$ and $3.9\,\text{mol kg}^{-1}$, respectively, this work; (– – –) (smoothed) prediction from Rumpf and Maurer [4,15]; (—) (smoothed) correlation, this work.

Table 1
Enthalpy change upon dilution $\Delta_{dil}H$ of $\{SO_2 + (NH_4)_2SO_4 + H_2O\}$ in $\{(NH_4)_2SO_4 + H_2O\}$

T (K)	$\bar{m}_{(NH_4)_2SO_4}$[a] (mol kg^{-1})	$\bar{m}^{(u)}_{SO_2}$ (mol kg^{-1})	$\tilde{m}^{(u)}$ (g)	$\tilde{m}^{(l)}$ (g)	$\Delta_{dil}H^{(exp)}$ (J)	$\Delta_{dil}H^{(corr)}$ (J)	$\Delta_{dil}H^{(pred)}$ (J)
312.7	0.968	1.799	28.059	17.175	−4.5 ± 2.1	−5.98	16.03
312.7	0.968	1.799	27.947	17.236	−3.8 ± 2.1	−5.97	16.10
312.7	0.968	1.799	28.068	17.147	−4.2 ± 2.1	−5.99	15.99
312.7	0.968	1.799	27.925	17.236	−4.1 ± 2.1	−5.97	16.09
312.7	0.968	1.799	27.936	17.220	−3.9 ± 2.1	−5.98	16.07
312.7	0.968	1.799	28.119	17.219	−4.0 ± 2.1	−5.99	16.07
312.6	0.968	1.799	27.917	17.151	−4.6 ± 2.1	−5.97	16.00
312.7	0.968	1.799	27.860	17.225	−4.1 ± 2.1	−5.97	16.08
312.7	1.053	3.810	29.089	17.265	−38.2 ± 2.8	−38.06	−17.11
312.7	1.053	3.810	28.946	17.314	−38.8 ± 2.8	−37.99	−16.95
312.7	1.053	3.810	29.227	17.284	−38.1 ± 2.8	−38.18	−17.23
312.7	1.053	3.810	28.984	17.319	−38.2 ± 2.8	−38.02	−16.98
312.7	1.053	3.810	29.123	17.305	−38.3 ± 2.8	−38.13	−17.12
312.7	1.053	3.810	29.532	17.321	−39.8 ± 2.8	−38.38	−17.45
312.7	3.962	1.784	31.222	19.321	13.2 ± 2.3	12.58	39.81
312.7	3.962	1.784	30.750	19.389	13.3 ± 2.3	12.59	39.95
312.7	3.962	1.784	31.395	19.307	13.1 ± 2.3	12.58	39.80
312.7	3.962	1.784	31.108	19.432	13.8 ± 2.3	12.64	40.03
312.7	3.962	1.784	31.236	19.327	13.2 ± 2.3	12.58	39.80
312.7	3.962	1.784	30.922	19.387	13.4 ± 2.3	12.60	39.92
312.7	3.962	1.784	31.487	19.328	14.1 ± 2.3	12.60	39.83
312.7	3.962	1.784	31.459	19.402	13.5 ± 2.3	12.64	40.02
312.7	3.741	3.421	31.294	19.213	10.1 ± 2.2	11.14	35.42
312.7	3.741	3.421	31.259	19.269	10.5 ± 2.2	11.19	35.61
312.7	3.741	3.421	31.492	19.222	9.1 ± 2.2	11.13	35.39
312.7	3.741	3.421	31.232	19.262	9.1 ± 2.2	11.20	35.62
351.6	0.950	2.080	27.893	17.095	−8.6 ± 2.2	−7.93	1.46
351.6	0.950	2.080	28.331	17.073	−8.7 ± 2.2	−7.97	1.37
351.6	0.950	2.080	28.318	17.083	−8.5 ± 2.2	−7.98	1.38
351.6	0.950	2.080	27.799	17.091	−7.7 ± 2.2	−7.93	1.45
351.6	0.950	2.080	28.216	17.086	−8.3 ± 2.2	−7.97	1.39
351.6	0.950	2.080	27.723	17.081	−8.4 ± 2.2	−7.93	1.41
351.6	0.986	3.332	28.534	17.170	−21.5 ± 2.4	−20.36	−22.00
351.7	0.986	3.332	28.061	17.179	−23.7 ± 2.5	−20.21	−21.76
351.6	0.986	3.332	28.301	17.344	−22.8 ± 2.5	−20.39	−21.86
351.6	0.986	3.332	28.647	17.197	−21.0 ± 2.4	−20.41	−22.11
351.6	3.691	2.042	30.993	19.055	5.1 ± 2.1	5.55	76.47
351.6	3.691	2.042	30.543	19.121	5.5 ± 2.1	5.53	76.54
351.6	3.691	2.042	30.578	19.057	6.5 ± 2.1	5.51	76.34
351.6	3.691	2.042	30.937	19.073	6.6 ± 2.1	5.54	76.52
351.6	3.691	2.042	30.571	19.057	7.5 ± 2.2	5.51	76.33
351.6	4.036	3.803	31.162	19.307	8.9 ± 2.2	9.59	90.15
351.7	4.036	3.803	30.902	19.272	9.1 ± 2.2	9.52	90.07
351.7	4.036	3.803	31.201	19.298	8.7 ± 2.2	9.56	90.12
351.7	4.036	3.803	31.009	19.264	7.3 ± 2.1	9.49	90.03
351.7	4.036	3.803	31.711	19.305	7.3 ± 2.1	9.56	90.05
351.7	4.036	3.803	31.110	19.268	6.2 ± 2.1	9.50	90.02

Experimental results$^{(exp)}$, correlation results$^{(corr)}$ (from the model presented here) and prediction results$^{(pred)}$ (from the model by Rumpf and Maurer [4]).

[a] $\bar{m}^{(u)}_{(NH_4)_2SO_4} = \bar{m}^{(l)}_{(NH_4)_2SO_4}$.

exothermic behavior is observed. As for ammonium sulfate, adding small amounts of sodium sulfate results in smaller absolute enthalpy changes, i.e., a shift towards endothermic behavior is observed. The experimental numbers for the enthalpy change range from about −26 to 5 J. The correction term resulting from $\int V\mathrm{d}p$ ranges from about −0.6 to about 2 J.

The absolute uncertainty in $\Delta_{dil}H$ is estimated to about $\pm(0.02|Q_{dil}| + 2\,\mathrm{J})$. The first contribution results from the uncertainty in the calibration experiments. The second contribution results from a Gauss error propagation calculation and accounts for uncertainties in temperature (T), salt molality in the upper and lower chamber ($\bar{m}_s$), gas molality in the upper chamber ($\bar{m}^{(u)}_{SO_2}$), the amounts of masses in the upper and the lower chamber ($\tilde{m}^{(u)}$, $\tilde{m}^{(l)}$), the work necessary to move the punching knife (W_{diss}), and the work required in the isothermal change of the volume during the mixing process ($\int V\mathrm{d}p$).

Table 2
Enthalpy change upon dilution $\Delta_{dil}H$ of $\{SO_2 + Na_2SO_4 + H_2O\}$ in $(Na_2SO_4 + H_2O)$

T (K)	$\bar{m}_{Na_2SO_4}$[a] (mol kg^{-1})	$\bar{m}^{(u)}_{SO_2}$ (mol kg^{-1})	$\tilde{m}^{(u)}$ (g)	$\tilde{m}^{(l)}$ (g)	$\Delta_{dil}H^{(exp)}$ (J)	$\Delta_{dil}H^{(corr)}$ (J)	$\Delta_{dil}H^{(pred)}$ (J)
312.7	0.969	2.082	28.963	17.898	−3.8 ± 2.1	−1.41	12.17
312.7	0.969	2.082	28.874	17.957	−3.5 ± 2.1	−1.37	12.16
312.7	0.969	2.082	29.215	17.883	−2.7 ± 2.1	−1.44	12.23
312.7	0.969	2.082	28.974	17.953	−2.5 ± 2.1	−1.39	12.18
312.7	0.969	2.082	28.680	17.863	−3.3 ± 2.1	−1.37	12.09
312.7	0.969	2.082	28.838	17.983	−2.3 ± 2.0	−1.36	12.16
312.7	0.969	2.082	29.145	17.870	−3.0 ± 2.1	−1.42	12.20
312.7	0.969	2.082	28.874	17.957	−3.5 ± 2.1	−1.37	12.16
312.6	1.006	3.775	30.047	18.012	−20.5 ± 2.4	−21.76	30.05
312.7	1.006	3.775	30.163	18.052	−22.8 ± 2.5	−21.78	30.05
312.6	1.006	3.775	29.977	17.997	−21.3 ± 2.4	−21.72	30.02
312.7	1.006	3.775	29.473	18.053	−21.5 ± 2.4	−21.47	30.00
312.7	1.006	3.775	29.889	18.010	−20.5 ± 2.4	−21.67	30.01
312.7	1.006	3.775	29.789	18.059	−20.9 ± 2.4	−21.62	30.04
312.6	1.006	3.775	29.640	17.992	−20.3 ± 2.4	−21.57	29.99
312.7	1.006	3.775	29.867	18.090	−20.2 ± 2.4	−21.69	30.12
312.7	1.006	3.775	30.169	18.312	−20.2 ± 2.4	−21.94	30.51
312.7	1.006	3.775	30.361	18.445	−20.4 ± 2.4	−22.05	30.68
312.6	1.246	1.866	29.920	18.473	2.5 ± 2.1	1.11	18.81
312.7	1.246	1.866	29.712	18.322	2.2 ± 2.0	1.12	18.67
312.6	1.246	1.866	29.977	18.446	2.7 ± 2.1	1.10	18.82
312.7	1.246	1.866	30.106	18.423	2.2 ± 2.0	1.10	18.85
312.7	1.246	1.866	29.767	18.313	3.4 ± 2.1	1.12	18.68
312.7	1.204	4.051	30.472	18.324	−18.2 ± 2.4	−18.67	72.25
312.7	1.204	4.051	30.270	18.401	−19.1 ± 2.4	−18.56	72.30
312.7	1.204	4.051	30.647	18.338	−18.1 ± 2.4	−18.74	72.38
312.7	1.204	4.051	30.475	18.387	−17.7 ± 2.4	−18.65	72.37
312.7	1.204	4.051	30.761	18.334	−18.1 ± 2.4	−18.77	72.40
312.7	1.204	4.051	30.695	18.391	−18.8 ± 2.4	−18.72	72.47
312.7	1.204	4.051	30.093	18.321	−19.3 ± 2.4	−18.51	72.04
312.7	1.204	4.051	30.321	18.408	−18.8 ± 2.4	−18.59	72.35
351.7	1.007	2.174	29.804	17.926	−5.9 ± 2.1	−1.60	−31.91
351.7	1.007	2.174	29.280	17.914	−6.7 ± 2.1	−1.57	−31.83
351.7	1.007	2.174	29.792	17.934	−5.6 ± 2.1	−1.60	−31.96
351.7	1.007	2.174	28.909	17.924	−5.3 ± 2.1	−1.55	−31.80
351.7	1.007	2.174	30.284	17.938	−5.4 ± 2.1	−1.62	−31.99
351.7	1.007	2.174	29.651	17.930	−4.8 ± 2.1	−1.59	−31.92
351.7	1.007	2.174	28.406	17.893	−5.9 ± 2.1	−1.52	−31.70
351.7	1.007	2.174	28.259	17.911	−5.7 ± 2.1	−1.52	−31.73
351.7	0.995	4.292	30.606	17.913	−24.6 ± 2.5	−30.28	−72.06
351.7	0.995	4.292	29.779	17.908	−26.4 ± 2.5	−29.75	−71.32
351.7	0.995	4.292	29.724	17.889	−23.4 ± 2.5	−29.71	−71.25
351.7	0.995	4.292	30.489	17.912	−24.9 ± 2.5	−30.22	−72.02
351.7	0.995	4.292	29.682	17.908	−23.5 ± 2.5	−29.70	−71.29
351.7	1.477	1.980	30.782	18.710	4.2 ± 2.1	0.23	−19.95
351.7	1.477	1.980	30.100	18.694	4.1 ± 2.1	0.19	−20.05
351.7	1.483	1.815	30.385	18.701	3.2 ± 2.1	−0.05	−20.80
351.7	1.483	1.815	30.951	18.713	3.4 ± 2.1	−0.04	−20.84
351.8	1.483	1.815	30.214	18.760	4.7 ± 2.1	−0.08	−20.94
351.7	1.483	1.815	30.950	18.699	4.2 ± 2.1	−0.01	−20.75
351.7	1.483	1.815	30.198	18.695	5.0 ± 2.1	−0.05	−20.80
351.7	1.483	1.815	30.823	18.710	4.3 ± 2.1	−0.04	−20.84
351.7	1.483	1.815	30.208	18.689	5.2 ± 2.1	−0.06	−20.83
351.7	1.419	3.706	31.383	18.586	−16.4 ± 2.3	−11.59	−21.55
351.7	1.419	3.706	30.811	18.608	−15.8 ± 2.3	−11.43	−21.54
351.7	1.419	3.706	30.223	18.586	−15.7 ± 2.3	−11.20	−21.31
351.7	1.419	3.706	31.196	18.615	−14.8 ± 2.3	−11.63	−21.90
351.7	1.419	3.706	30.708	18.611	−14.7 ± 2.3	−11.38	−21.48
351.7	1.419	3.706	31.238	18.625	−14.4 ± 2.3	−11.62	−21.83
351.7	1.419	3.706	30.717	18.610	−14.1 ± 2.3	−11.41	−21.57
351.8	1.419	3.706	31.253	18.617	−13.2 ± 2.3	−11.74	−22.24

Experimental results$^{(exp)}$, correlation results$^{(corr)}$ (from the model presented here) and prediction results$^{(pred)}$ (from the model by Rumpf and Maurer [4]).

[a] $\bar{m}^{(u)}_{Na_2SO_4} = \bar{m}^{(l)}_{Na_2SO_4}$.

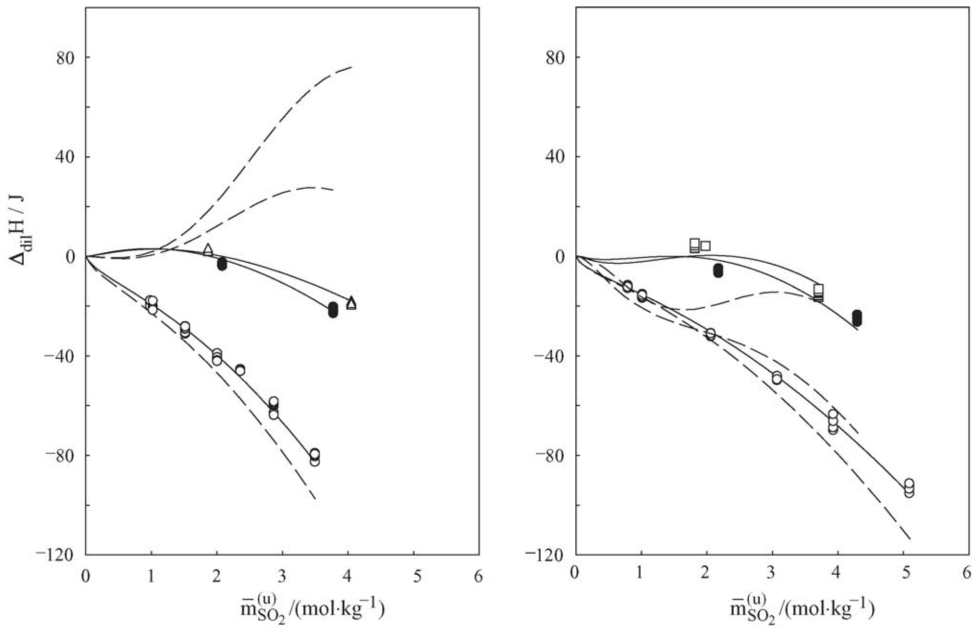

Fig. 2. Enthalpy change upon dilution of about 30 g ($SO_2 + Na_2SO_4 + H_2O$) with about 18.3 g ($Na_2SO_4 + H_2O$) at equal stoichiometric salt molality $\bar{m}_{Na_2SO_4}$ in the upper and lower chamber, plotted against the stoichiometric molality of the gas in the upper chamber ($\bar{m}_{SO_2}^{(u)}$) (T = 312.7 K in the left diagram, T = 351.7 K in the right diagram). Experimental results: (○)$\bar{m}_{Na_2SO_4} = 0$ (from ref. [5]), (●,△,□)$\bar{m}_{Na_2SO_4} \approx 1$, 1.2, and 1.45 mol kg^{-1}, respectively, this work; (– – –) (smoothed) prediction from Rumpf and Maurer [4,15]; (—) (smoothed) correlation, this work.

4. Thermodynamic modeling

4.1. Chemical reaction equilibrium in aqueous solutions of SO_2 and {$(NH_4)_2SO_4$ or Na_2SO_4}

When sufficiently small amounts of the strong electrolytes ammonium sulfate or sodium sulfate are added to pure liquid water, that salts can be regarded as fully dissociated:

$$M_2SO_4(s) \rightarrow 2M^+(aq) + SO_4{}^{2-}(aq),$$

where M = NH_4 or Na. When the gas sulfur dioxide is dissolved in an aqueous solution the following (reversible) chemical reactions are considered in that liquid: the formation of bisulfite ($HSO_3{}^-$), sulfite ($SO_3{}^{2-}$), and pyrosulfite ($S_2O_5{}^{2-}$) (cf. Goldberg and Parker [10]):

$$SO_2(aq) + H_2O(l) \rightleftharpoons H^+(aq) + HSO_3{}^-(aq), \tag{I}$$

$$HSO_3{}^-(aq) \rightleftharpoons H^+(aq) + SO_3{}^{2-}(aq), \tag{II}$$

$$2HSO_3{}^-(aq) \rightleftharpoons S_2O_5{}^{2-}(aq) + H_2O(l), \tag{III}$$

i.e., sulfur dioxide dissolves in that liquid not only in molecular, but also in non-volatile, ionic form. Furthermore, the autoprotolysis of water has to be considered:

$$H_2O(l) \rightleftharpoons H^+(aq) + OH^-(aq) \tag{IV}$$

Due to the sour character of aqueous solutions of sulfur dioxide, adding one of the aforementioned salts {$(NH_4)_2SO_4$ or Na_2SO_4} to that solution results in a partial protonation of sulfate to bisulfate:

$$SO_4{}^{2-}(aq) + H^+(aq) \rightleftharpoons HSO_4{}^-(aq) \tag{V}$$

The condition for chemical equilibrium for a chemical reaction r is expressed as:

$$K_r(T) = \prod_i a_i^{\nu_{i,r}} \tag{3}$$

The influence of pressure on a chemical reaction equilibrium constant (K_r) is neglected here, a_i is the activity of species i. The reference state for the chemical potential of the solvent (water) is the pure liquid at systems temperature and pressure, whereas for the chemical potential of a solute species it is the one molal solution of that solute in pure water at systems temperature and pressure, the solute experiencing the same interactions as if it is infinitely diluted in pure water. $\nu_{i,r}$ is the stoichiometric factor of reactant i in reaction r ($\nu_{i,r} > 0$ for a product and $\nu_{i,r} < 0$ for an educt).

The balance equations for the amounts-of-substance of a species i in the liquid solution is:

$$n_i = \bar{n}_i + \sum_r \nu_{i,r}\xi_r \tag{4}$$

where ξ_r is the extent of reaction r. Solving this set of equations for a given temperature and given stoichiometric amounts-of-substances $\bar{n}_i$ of components [i.e., SO_2, H_2O, Na^+, $NH_4{}^+$, and $SO_4{}^{2-}$] results in the speciation, i.e., the "true" composition of the liquid phase (the amounts-of-substances n_i of all species).

4.2. Gibbs excess energy model

Activity coefficients of solute species were calculated from Pitzer's equation for the excess Gibbs energy (G^{E}) of aqueous electrolyte solutions [11,12]:

$$\frac{G^E}{M_{\mathrm{W}}^{*} n_{\mathrm{W}} RT} = f(I) + \sum_{i,j\neq \mathrm{W}} \sum \frac{m_i}{m^\circ}\frac{m_j}{m^\circ}\lambda_{ij}(I) + \sum_{i,j,k\neq \mathrm{W}} \sum\sum \frac{m_i}{m^\circ}\frac{m_j}{m^\circ}\frac{m_k}{m^\circ}\mu_{ijk}. \quad (5)$$

M_{W}^{*} is the molar mass of water divided by 1000 g mol^{-1} ($M_{\mathrm{W}}^{*} = 0.01801528$), n_{W} is the amounts-of-substance of water, R is the universal gas constant, T is the absolute temperature, m_i is the molality of solute species i, i.e., the amounts-of-substance n_i of this species i per kilogram of water, and $m^\circ = 1\ \mathrm{mol\,kg^{-1}}$. $f(I)$ is Pitzer's modification of the Debye-Hückel term. The activity coefficient of a solute species (on the molality scale) is directly calculated from Eq. (5), whereas the activity of water is calculated from the activity coefficients of all solute species by applying the Gibbs–Duhem equation. As usual, binary and ternary osmotic virial coefficients in Pitzer's G^{E} equation are treated as symmetric:

$$\lambda_{ij} = \lambda_{ji}, \quad (6)$$

$$\mu_{ijk} = \mu_{ikj} = \mu_{jik} = \mu_{jki} = \mu_{kij} = \mu_{kji}. \quad (7)$$

"Symmetrical and unsymmetrical mixing terms" [12] as well as all parameters describing interactions between ionic species carrying charges of the same sign were neglected.

According to Pitzer's equations, λ_{ij} is written as:

$$\lambda_{ij} = \beta_{ij}^{(0)} + \beta_{ij}^{(1)} g(\alpha_{ij}^{(1)}\sqrt{I}) + \beta_{ij}^{(2)} g(\alpha_{ij}^{(2)}\sqrt{I}), \quad (8)$$

where the ionic strength of the solution is given by:

$$I = \frac{1}{2}\sum_i \frac{m_i}{m^\circ} z_i^2 \quad (9)$$

(z_i is the number of charges on the solute i).

$g(x)$ is defined as:

$$g(x) = \frac{2}{x^2}[1 - (1 + x)\exp(-x)]. \quad (10)$$

$\beta_{ij}^{(0)}$, $\beta_{ij}^{(1)}$, $\beta_{ij}^{(2)}$, $\alpha_{ij}^{(1)}$, and $\alpha_{ij}^{(2)}$ are binary parameters. In the present work, $\alpha_{ij}^{(1)}$ is set to 2. Furthermore, $\beta_{ij}^{(2)}$ is set to zero, therefore, $\alpha_{ij}^{(2)}$ is not required.

When a single (chemically non-reacting) gas G is dissolved in pure water, the model contains only two interaction parameters ($\beta_{G,G}^{(0)}$ and $\mu_{G,G,G}$).

For binary (chemically non-reacting) systems (water + strong electrolyte $\mathrm{M}_{\nu+}\mathrm{X}_{\nu-}$) it is not possible to separate the influence of $\mu_{\mathrm{M,M,X}}$ from that of $\mu_{\mathrm{M,X,X}}$. Therefore, both ternary parameters are usually summarized in C_{MX}^{ϕ}:

$$C_{\mathrm{MX}}^{\phi} = \frac{3}{\sqrt{\nu_+\nu_-}}[\nu_+\mu_{\mathrm{M,M,X}} + \nu_-\mu_{\mathrm{M,X,X}}] \quad (11)$$

It is common practice to report $\beta_{\mathrm{M,X}}^{(0)}$, $\beta_{\mathrm{M,X}}^{(1)}$, and C_{MX}^{ϕ} (or to set either $\mu_{\mathrm{M,M,X}}$ or $\mu_{\mathrm{M,X,X}}$ to zero and report either $\mu_{\mathrm{M,X,X}}$ or $\mu_{\mathrm{M,M,X}}$).

In ternary (chemically non-reacting) systems (water + strong electrolyte $\mathrm{M}_{\nu+}\mathrm{X}_{\nu-}$ + gas G) it is similarly not possible to separate the influence of M on solute G from that of X on solute G. Therefore, it is common practice to use the following comprehensive parameters:

$$B_{G,\mathrm{MX}}^{(j)} = \nu_+\beta_{G,\mathrm{M}}^{(j)} + \nu_-\beta_{G,\mathrm{X}}^{(j)} \quad j = 0, 1 \quad (12)$$

$$\Gamma_{G,\mathrm{MX,MX}} = \nu_+^2\mu_{G,\mathrm{M,M}} + 2\nu_+\nu_-\mu_{G,\mathrm{M,X}} + \nu_-^2\mu_{G,\mathrm{X,X}} \quad (13)$$

$$\Gamma_{G,G,\mathrm{MX}} = \nu_+\mu_{G,G,\mathrm{M}} + \nu_-\mu_{G,G,\mathrm{X}} \quad (14)$$

$B_{G,\mathrm{MX}}^{(1)}$ is rarely needed to describe the solubility of a gas in an aqueous solution of a strong electrolyte. $B_{G,\mathrm{MX}}^{(0)}$, $\Gamma_{G,\mathrm{MX,MX}}$, $\Gamma_{G,G,\mathrm{MX}}$ are usually sufficient for a good description of gas solubility. In $B_{G,\mathrm{MX}}^{(0)}$, arbitrarily either $\beta_{G,\mathrm{M}}^{(0)}$ or $\beta_{G,\mathrm{X}}^{(0)}$ may be set to zero; in $\Gamma_{G,\mathrm{MX,MX}}$, one can arbitrarily set two of the three parameters $\mu_{G,\mathrm{M,M}}$, $\mu_{G,\mathrm{M,X}}$ and $\mu_{G,\mathrm{X,X}}$ to zero; and in $\Gamma_{G,G,\mathrm{MX}}$, one can arbitrarily set either $\mu_{G,G,\mathrm{M}}$ or $\mu_{G,\mathrm{X,X}}$ to zero.

4.3. Enthalpy change upon dilution

The enthalpy change upon mixing of two liquid solutions [or upon diluting one liquid solution {superscript (u)} by another liquid solution {superscript (l)}] can generally be expressed as:

$$\Delta_{\mathrm{dil}}H = \sum_i n_i^{(2)}h_i^{(2)} - \sum_i n_i^{(u)}h_i^{(u)} - \sum_i n_i^{(l)}h_i^{(l)} \quad (15)$$

where $n_i^{(u)}$ and $n_i^{(l)}$ are the true amounts-of-substances of species i in the upper and lower chambers of the cell before mixing (state 1), respectively, and $n_i^{(2)}$ is the true amounts-of-substance of species i after mixing (state 2). h_i is the partial molar enthalpy of species i. Combining the mass balance on the stoichiometric components:

$$\bar{n}_i^{(2)} = \bar{n}_i^{(u)} + \bar{n}_i^{(l)} \quad (16)$$

with Eq. (4) gives for the true species:

$$n_i^{(2)} = n_i^{(u)} + n_i^{(l)} + \sum_r \nu_{i,r}\Delta\xi_r, \quad (17)$$

where:

$$\Delta\xi_r = \xi_r^{(2)} - \xi_r^{(u)} - \xi_r^{(l)}. \quad (18)$$

Combining Eqs. (15) and (17) with:

$$h_i = h_i^{(\mathrm{ref})} + h_i^E \quad (19)$$

(where (ref) and E stand for a reference and an excess property, respectively) results in:

$$\Delta_{\text{dil}} H = \sum_i n_i^{(u)} (h_i^{E,(2)} - h_i^{E,(u)}) + \sum_i n_i^{(l)} (h_i^{E,(2)} - h_i^{E,(l)}) + \sum_r \Delta\xi_r [\Delta_r h^{(\text{ref})} + \sum_i \nu_{i,r} h_i^{E,(2)}]. \tag{20}$$

Pitzer's expressions for the activity coefficient of a solute i (γ_i) and for the activity of the solvent water (a_W) are used to calculate the partial molar excess enthalpies h_i^E and h_W^E:

$$h_i^E = -RT^2 \left(\frac{\partial \ln \gamma_i}{\partial T}\right)_{p,n_j}, \tag{21}$$

$$h_W^E = -RT^2 \left(\frac{\partial \ln a_W}{\partial T}\right)_{p,n_j}. \tag{22}$$

The molar reaction enthalpy:

$$\Delta_r H = \Delta_r h^{(\text{ref})} = \sum_i \nu_{i,r} h_i^{(\text{ref})} \tag{23}$$

is calculated from the temperature dependent chemical reaction equilibrium constant:

$$\Delta_r H = -R \frac{\mathrm{d} \ln K_r}{\mathrm{d}(1/T)}. \tag{24}$$

These equations are straightforward applied to the dilution process considered in the present work.

4.4. Vapor–liquid equilibrium

The phase equilibrium condition for the solubility of sulfur dioxide in water results in the extended Henry's law for SO_2:

$$k_{\text{H},SO_2} \exp\left[\frac{v_{SO_2}^{(\infty)}(p - p_W^s)}{RT}\right] \frac{m_{SO_2}}{m^\circ} \gamma_{SO_2} = y_{SO_2} p \phi_{SO_2} \tag{25}$$

and in the extended Raoult's law for water:

$$p_W^s \phi_W^s \exp\left[\frac{v_W(p - p_W^s)}{RT}\right] a_W = y_W p \phi_W \tag{26}$$

From these equations, the total pressure p and the vapor phase composition (y_i is the mole fraction of component i in the vapor phase) are calculated. $k_{\text{H},SO_2}(T)$ is Henry's constant of sulfur dioxide in pure water (based on the molality scale) at the vapor pressure of pure water (p_W^s). $v_{SO_2}^{(\infty)}$ and v_W are the partial molar volume of sulfur dioxide infinitely diluted in water and the molar volume of liquid water, respectively. ϕ_i is the vapor phase fugacity coefficient of component i.

Table 4
Henry's constant of sulfur dioxide in water (on the molality scale) [15]

A	B	C	D	T (K)
−154.827	321.17	29.872	−0.0634	293–393

$\ln\left[\frac{k_{\text{H},SO_2}}{\text{MPa}}\right] = A + \frac{B}{(T/\text{K})} + C \ln(T/\text{K}) + D(T/\text{K}).$

4.5. Required thermodynamic properties

The temperature dependent chemical reaction equilibrium constants K_r (r = I–V) were obtained from the literature [1,10,13,14] (cf., Table 3). The correlation equation for Henry's constant $k_{\text{H},SO2}$ in water applied in the present work [15] is given in Table 4. The dielectric constant as well as the density of pure water are required for the calculation of Pitzer's modification of the Debye–Hückel term. They were approximated by the properties of pure, saturated liquid water [16,17]. The vapor pressure of pure water (p_W^s) was calculated from the equation by Saul and Wagner [17]. The partial molar volumes of the dissolved gases ($v_i^{(\infty)}$) were calculated as recommended by Brelvi and O'Connell [18] (details are given in refs. [5,19]). The vapor phase fugacity coefficients (ϕ_i) were calculated from the virial equation of state which was truncated after the second virial coefficient (for details, cf. refs. [5,20]).

Within the concentration ranges of sulfur dioxide and (ammonium sulfate or sodium sulfate) considered in the present work, no second condensed phase {neither, e.g., a (sulfur dioxide rich) liquid phase (cf., e.g., Rumpf and Maurer [4,15]), nor any salt precipitation, e.g., of $(NH_4)_2SO_4$, $(NH_4)_2S_2O_5$, Na_2SO_4, $Na_2S_2O_5$, etc. (cf., e.g., Pereda et al. [21])} has to be considered. Therefore, it was not necessary to extend the model in order to allow for the appearance of those additional phases.

5. Correlation

Fig. 3 shows calculation results for the speciation (at T = 353 K) in aqueous solutions of the single salts ammonium sulfate {$\bar{m}_{(NH_4)_2SO_4}$ = 4 mol kg^{-1}, left diagram} and sodium sulfate ($\bar{m}_{Na_2SO_4}$ = 1 mol kg^{-1}, right diagram), when

Table 3
Chemical reaction equilibrium constants (on the molality scale)

Reaction r	A	B	C	10^2D	T (K)	Source
I	554.977	−16700.5	−93.6745	10.2231	278–393	[10]
II	−358.577	5477.29	65.3084	−16.2367	278–393	[10]
III	−10.226	2123.6	–	–	313–353	[1]
IV	140.932	−13445.9	−22.4773	–	273–498	[13]
V	14.0321	−2825.2	–	–	∼298	[14]

$\ln K_r = A + \frac{B}{(T/\text{K})} + C \ln(T/\text{K}) + D(T/\text{K}).$

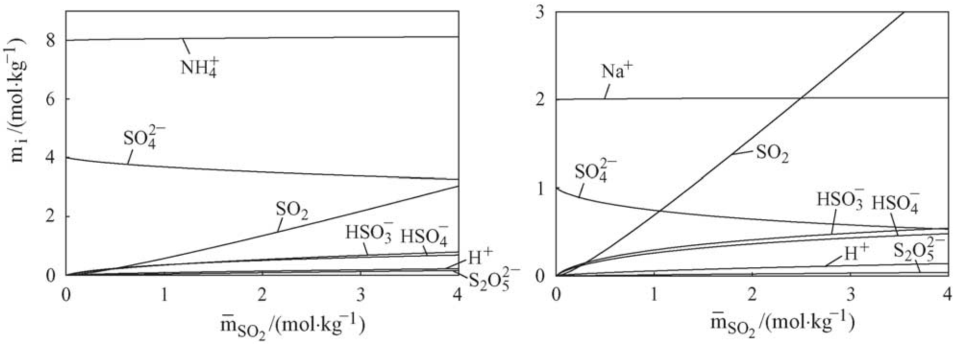

Fig. 3. Speciation in the systems $\{SO_2 + (NH_4)_2SO_4 + H_2O\}$ $\{\bar{m}_{(NH_4)_2SO_4} = 4\,\mathrm{mol\,kg^{-1}}$, left diagram$\}$ and $(SO_2 + Na_2SO_4 + H_2O)$ ($\bar{m}_{Na_2SO_4} = 1\,\mathrm{mol\,kg^{-1}}$, right diagram) at 353.15 K. Activities of all species were estimated from Pitzer's Debye Hückel term alone.

sulfur dioxide is added. The activities of all species were estimated from Pitzer's Debye–Hückel term alone, i.e., the calculated speciation is only approximative. The amounts of water and sulfur dioxide in those liquid mixtures, which are converted to OH^- and SO_3^{2-} ions are negligibly small. The liquid mixture $(SO_2 + M_2SO_4 + H_2O)$, with M = NH_4 or Na, can be regarded as an aqueous solution of the single gas SO_2, and the eight strong electrolytes M_2SO_4, $MHSO_4$, $MHSO_3$, $M_2S_2O_5$, H_2SO_4, HX (with X = HSO_4 and HSO_3), and $H_2S_2O_5$. The properties of liquid mixtures of $(SO_2 + M_2SO_4 + H_2O)$ might therefore be described with parameters for interactions which also occur in the binary subsystems $(SO_2 + H_2O)$, (strong electrolyte + H_2O), and (SO_2 + strong electrolyte + H_2O), with the aforementioned strong electrolytes.

6. Interaction parameters in Pitzer's G^E-equation

6.1. $(SO_2 + H_2O)$ system

As already discussed in previous publications [5,15], when dissolving sulfur dioxide in pure water, the amounts of the gas reacting with water, according to reactions I–IV to form ionic species is negligibly small (disregarding highly diluted solutions), i.e., dissolved sulfur dioxide is predominantly present in molecular (rather than in ionic) form. Therefore, in order to correlate thermodynamic properties of that binary system, parameters describing interactions between SO_2 and the ionic species H^+, $HSO_3{}^-$, $SO_3{}^{2-}$, $S_2O_5{}^{2-}$, and OH^- as well as between those ionic species can be neglected. The correlation equations for the (temperature dependent) Pitzer parameters describing interactions between SO_2 molecules in water ($\beta^{(0)}_{SO_2,SO_2}$ and μ_{SO_2,SO_2,SO_2}) were adopted from Pérez-Salado Kamps et al. [5]. They are based on the gas solubility data reported by Rumpf and Maurer [15] (for temperatures from 293 K to 393 K) as well as on the data for the enthalpy of dilution given in ref. [5] (at T ≈ 313 K and 352 K). $\beta^{(0)}_{SO_2,SO_2}$ proved sufficient to describe all experimental data within experimental accuracy, i.e., μ_{SO_2,SO_2,SO_2} was set to zero (see Table 5). Those parameters are valid up to the solubility limit of SO_2 in water (i.e., up to the formation of a second SO_2-rich liquid phase).

6.2. $\{(NH_4)_2SO_4 + H_2O\}$ system

The correlation equations for the three (temperature dependent) Pitzer parameters describing interactions between $NH_4{}^+$ and $SO_4{}^{2-}$ in aqueous solutions ($\beta^{(0)}_{NH_4{}^+,SO_4{}^{2-}}$, $\beta^{(1)}_{NH_4{}^+,SO_4{}^{2-}}$, and $C^{\phi}_{(NH_4)_2SO_4}$) were adopted from Rumpf et al. [6]. They are based on the numerical values for those parameters reported by Pitzer [12] for $T = 298.15$ K {which are based on isopiestic data up to saturation at that temperature (5.82 mol kg^{-1}) from Filippov et al. [22]} and on the data for the enthalpy of dilution given by Rumpf et al. [6] (at stoichiometric salt molalities up to about 5 mol kg^{-1} and temperatures from 313 to 373 K). Table 5 gives the correlation equations for $\beta^{(0)}_{NH_4{}^+,SO_4{}^{2-}}$, $\beta^{(1)}_{NH_4{}^+,SO_4{}^{2-}}$, and $\mu_{NH_4{}^+,NH_4{}^+,SO_4{}^{2-}} = \frac{\sqrt{2}}{6}C^{\phi}_{(NH_4)_2SO_4}$, where $\mu_{NH_4{}^+,SO_4{}^{2-},SO_4{}^{2-}}$ was set to zero.

6.3. $(NH_4HSO_3 + H_2O)$, $\{(NH_4)_2S_2O_5 + H_2O)$, $(SO_2 + NH_4HSO_3 + H_2O)$, and $\{SO_2 + (NH_4)_2S_2O_5 + H_2O\}$ systems

Pitzer's method requires the following (temperature dependent) parameters describing interactions in those aqueous solutions: (1) for interactions between $NH_4{}^+$ and $HSO_3{}^-$: $\beta^{(0)}_{NH_4{}^+,HSO_3{}^-}$, $\beta^{(1)}_{NH_4{}^+,HSO_3{}^-}$, and $C^{\phi}_{NH_4HSO_3}$, (2) for interactions between $NH_4{}^+$ and $S_2O_5{}^{2-}$: $\beta^{(0)}_{NH_4{}^+,S_2O_5{}^{2-}}$, $\beta^{(1)}_{NH_4{}^+,S_2O_5{}^{2-}}$, and $C^{\phi}_{(NH_4)_2S_2O_5}$, (3) for interactions between SO_2, $NH_4{}^+$ and $HSO_3{}^-$: $B^{(0)}_{SO_2,NH_4HSO_3}$, $\Gamma_{SO_2,NH_4HSO_3,NH_4HSO_3}$, and $\Gamma_{SO_2,SO_2,NH_4HSO_3}$, and (4) for interactions between SO_2, $NH_4{}^+$ and $S_2O_5{}^{2-}$: $B^{(0)}_{SO_2,(NH_4)_2S_2O_5}$, $\Gamma_{SO_2,(NH_4)_2S_2O_5,(NH_4)_2S_2O_5}$, and $\Gamma_{SO_2,SO_2,(NH_4)_2S_2O_5}$. When Pitzer's G^E-equation is applied to chemical reacting systems, for computational reasons, it is much easier to use the general equations for the activity coefficient of a solute species (and for the activity of water) as a function of the parameters $\beta^{(0)}_{ij}$, $\beta^{(1)}_{ij}$, and μ_{ijk}, rather than using rearranged

Table 5
Interaction Parameters in Pitzer's equation for the Gibbs excess energy

Parameter	q_1	q_2	q_3	q_4	q_5	T (K)	Determined from experimental results for the subsystem
$\beta^{(0)}_{SO_2,SO_2}$	0.10922	−140.72	30216			293–393	$SO_2 + H_2O$ [5]
$\beta^{(0)}_{NH_4{}^+,SO_4{}^{2-}}$	17.79712	−589.017		–2.979609	0.004005157	298–373	$(NH_4)_2SO_4 + H_2O$ [6][a]
$\beta^{(1)}_{NH_4{}^+,SO_4{}^{2-}}$	766.00035	−23129.6		–130.631	0.189579		
$\mu_{NH_4{}^+,NH_4{}^+,SO_4{}^{2-}}$	−0.0444421	3.39601		0.00578395			
$\beta^{(0)}_{NH_4{}^+,HSO_3{}^-}$	0.016255	−3.5719				308–373	$SO_2 + NH_3 + H_2O$ [5]
$\beta^{(1)}_{NH_4{}^+,HSO_3{}^-}$	1.223	−545.1					
$\beta^{(0)}_{NH_4{}^+,S_2O_5{}^{2-}}$	0.335	−69.82					
$\beta^{(0)}_{SO_2,HSO_3{}^-}$	0.022057						
$\mu_{SO_2,NH_4{}^+,HSO_3{}^-}$	0.0025908	−1.2046					
$\mu_{SO_2,SO_2,HSO_3{}^-}$	0.0093098	−3.1034					
$\beta^{(0)}_{H^+,SO_4{}^{2-}}$	−0.32806	98.607				∼298	$H_2SO_4 + H_2O$ [14]
$\mu_{H^+,H^+,SO_4{}^{2-}}$	0.05971	−14.878					
$\beta^{(0)}_{H^+,HSO_4{}^-}$	0.05584	46.04					
$\beta^{(1)}_{H^+,HSO_4{}^-}$	−0.65758	336.514					
$\beta^{(0)}_{NH_4{}^+,HSO_4{}^-}$	0.0075					313–393	$SO_2 + (NH_4)_2SO_4 + H_2O^{\text{this work}}$
$\beta^{(1)}_{NH_4{}^+,HSO_4{}^-}$	−6.5899	2735.1					
$\beta^{(0)}_{SO_2,HSO_4{}^-}$	0.45514	−138.14					
$\beta^{(0)}_{SO_2,SO_4{}^{2-}}$	0.026315						
$\beta^{(0)}_{Na^+,SO_4{}^{2-}}$	correlation equations from ref. [27]					298–473	$Na_2SO_4 + H_2O$ [27]
$\beta^{(1)}_{Na^+,SO_4{}^{2-}}$							
$\mu_{Na^+,Na^+,SO_4{}^{2-}}$							
$\beta^{(0)}_{Na^+,HSO_3{}^-}$	−0.04625	3.875				313–353	$Na_2S_2O_5 + H_2O$ [1]
$\beta^{(0)}_{Na^+,S_2O_5{}^{2-}}$	0.1236	−40.55					
$\beta^{(0)}_{Na^+,HSO_4{}^-}$	0.034705	−14.839				313–393	$SO_2 + Na_2SO_4 + H_2O^{\text{this work}}$
$\beta^{(1)}_{Na^+,HSO_4{}^-}$	−6.2847	2706.5					
$\beta^{(0)}_{SO_2,Na^+}$	−0.041477	27.466					
$\mu_{SO_2,Na^+,SO_4{}^{2-}}$	−0.068316	24.363					

$f(T) = q_1 + \frac{q_2}{(T/\mathrm{K})} + \frac{q_3}{(T/\mathrm{K})^2} + q_4 \ln(T/\mathrm{K}) + q_5(T/\mathrm{K})$.

[a] Note that there are some typographical errors in the numerical values reported by Rumpf et al. [6].

equations as a function of comprehensive parameters {e.g., C^{ϕ}_{MX}, $B^{(0)}_{G,MX}$, $\Gamma_{G,MX,MX}$, $\Gamma_{G,G,MX}$ (cf. Eqs. (11)–(14))}. Of course, such a procedure does not increase the amount of independent parameters. Six parameters of the kind $\beta^{(0)}_{ij}$, $\beta^{(1)}_{ij}$, and μ_{ijk} ($\beta^{(0)}_{NH_4{}^+,HSO_3{}^-}$, $\beta^{(1)}_{NH_4{}^+,HSO_3{}^-}$, $\beta^{(0)}_{NH_4{}^+,S_2O_5{}^{2-}}$, $\beta^{(0)}_{SO_2,HSO_3{}^-}$, $\mu_{SO_2,NH_4{}^+,HSO_3{}^-}$, and $\mu_{SO_2,SO_2,HSO_3{}^-}$) describing interactions in these aqueous systems were adopted from Pérez-Salado Kamps et al. [5] (cf., Table 5). They are based on the gas solubility data for the system $(NH_3 + SO_2 + H_2O)$ reported by Rumpf et al. [23] (for $T \approx 313$ to 373 K) and by Johnstone [24] (for $T \approx 308$ to 363 K) as well as on experimental results for the enthalpy of dilution in that system given in [5] (at $T \approx 313$ and 352 K). The remaining parameters ($\mu_{NH_4{}^+,NH_4{}^+,HSO_3{}^-}$, $\mu_{NH_4{}^+,HSO_3{}^-,HSO_3{}^-}$, $\beta^{(1)}_{NH_4{}^+,S_2O_5{}^{2-}}$, $\mu_{NH_4{}^+,NH_4{}^+,S_2O_5{}^{2-}}$, $\mu_{NH_4{}^+,S_2O_5{}^{2-},S_2O_5{}^{2-}}$, $\beta^{(0)}_{SO_2,NH_4{}^+}$, $\mu_{SO_2,NH_4{}^+,NH_4{}^+}$, $\mu_{SO_2,HSO_3{}^-,HSO_3{}^-}$, $\mu_{SO_2,SO_2,NH_4{}^+}$, $\beta^{(0)}_{SO_2,S_2O_5{}^{2-}}$, $\mu_{SO_2,NH_4{}^+,S_2O_5{}^{2-}}$, $\mu_{SO_2,S_2O_5{}^{2-},S_2O_5{}^{2-}}$, and $\mu_{SO_2,SO_2,S_2O_5{}^{2-}}$) were not required in that correlation and were all set to zero.

6.4. $(H_2SO_4 + H_2O)$ system

The correlation equations for the (temperature dependent) Pitzer parameters describing interactions between H^+ and $SO_4{}^{2-}$ as well as between H^+ and $HSO_4{}^-$ in aqueous solutions {($\beta^{(0)}_{H^+,SO_4{}^{2-}}$, $\beta^{(1)}_{H^+,SO_4{}^{2-}}$, $C^{\phi}_{H_2SO_4}$) and ($\beta^{(0)}_{H^+,HSO_4{}^-}$, $\beta^{(1)}_{H^+,HSO_4{}^-}$, $C^{\phi}_{HHSO_4}$), respectively} were taken from Pitzer et al. [14]. They were determined from electromotive force data, isopiestic data as well as from heat of dilution measurements at temperatures around 298 K and sulfuric acid concentrations up to 6 mol kg^{-1}. Additional experimental and theoretical investigations on the thermodynamic properties of aqueous sulfuric acid solutions have been presented during the last decades (cf., e.g., Holmes and Mesmer [25] or Clegg et al. [26]). But due to the rather small amounts of H^+ species dissolved in the liquid mixtures under consideration in the present work, we refrained from extending Pitzer's G^E-equation (in order to account for unsymmetrical mixing terms and/or ionic strength dependent third virial coefficients), and therefore retained the correlation from Pitzer et al. [14]. Table 5 gives the correlation equations for $\beta^{(0)}_{H^+,SO_4{}^{2-}}$, $\mu_{H^+,H^+,SO_4{}^{2-}} = \frac{\sqrt{2}}{6} C^{\phi}_{H_2SO_4}$, $\beta^{(0)}_{H^+,HSO_4{}^-}$, and $\beta^{(1)}_{H^+,HSO_4{}^-}$. The parameters $\beta^{(1)}_{H^+,SO_4{}^{2-}}$, $\mu_{H^+,SO_4{}^{2-},SO_4{}^{2-}}$, and $C^{\phi}_{HHSO_4}$ (i.e., $\mu_{H^+,H^+,HSO_4{}^-}$ and $\mu_{H^+,HSO_4{}^-,HSO_4{}^-}$) were all set to zero.

6.5. Systems $(HX + H_2O)$, $(H_2S_2O_5 + H_2O)$, $(SO_2 + HX + H_2O)$, $(SO_2 + H_2S_2O_5 + H_2O)$, $(SO_2 + H_2SO_4 + H_2O)$, and $(SO_2 + HY + H_2O)$, where $X = HSO_3$ and $Y = HSO_4$

All parameters $\beta^{(0)}_{ij}$, $\beta^{(1)}_{ij}$, and μ_{ijk} for interactions between H^+ and all other solute species of these subsystems – with the exception of the parameters given in the previous section – were set to zero. This is justified by the rather small amounts of the H^+ species present in the liquid mixtures under consideration.

6.6. $(NH_4HSO_4 + H_2O)$, $\{SO_2 + (NH_4)_2SO_4 + H_2O\}$, and $(SO_2 + NH_4HSO_4 + H_2O)$ systems

Pitzer's method requires the following (temperature dependent) parameters describing interactions in those aqueous solutions: (1) for interactions between $NH_4{}^+$ and $HSO_4{}^-$: $\beta^{(0)}_{NH_4{}^+,HSO_4{}^-}$, $\beta^{(1)}_{NH_4{}^+,HSO_4{}^-}$, and $C^{\phi}_{NH_4HSO_4}$, (2) for interactions between SO_2, $NH_4{}^+$, and $SO_4{}^{2-}$: $B^{(0)}_{SO_2,(NH_4)_2SO_4}$, $\Gamma_{SO_2,(NH_4)_2SO_4,(NH_4)_2SO_4}$, and $\Gamma_{SO_2,SO_2,(NH_4)_2SO_4}$, and (3) for interactions between SO_2, $NH_4{}^+$, and $HSO_4{}^-$: $B^{(0)}_{SO_2,NH_4HSO_4}$, $\Gamma_{SO_2,NH_4HSO_4,NH_4HSO_4}$, and $\Gamma_{SO_2,SO_2,NH_4HSO_4}$. For the reasons explained before, only parameters of the kind $\beta^{(0)}_{ij}$, $\beta^{(1)}_{ij}$, and μ_{ijk} were considered. They were simultaneously fitted to the experimental results for the solubility of SO_2 in $\{(NH_4)_2SO_4 + H_2O\}$ reported by Rumpf and Maurer [4] (for $T \approx 333$–393 K) and to the new experimental results for the heat of dilution in that system from the present work (at $T \approx 313$ and 352 K). In an optimization procedure, the difference between experimental and calculated results for the total pressure as well as for the enthalpy of dilution was minimized. Four parameters, $\beta^{(0)}_{NH_4{}^+,HSO_4{}^-}$, $\beta^{(1)}_{NH_4{}^+,HSO_4{}^-}$, $\beta^{(0)}_{SO_2,HSO_4{}^-}$ and $\beta^{(0)}_{SO_2,SO_4{}^{2-}}$ (given in Table 5) proved sufficient to describe the experimental results almost within experimental uncertainty, i.e., $\mu_{NH_4{}^+,NH_4{}^+,HSO_4{}^-}$, $\mu_{NH_4{}^+,HSO_4{}^-,HSO_4{}^-}$, $\mu_{SO_2,NH_4{}^+,HSO_4{}^-}$, $\mu_{SO_2,HSO_4{}^-,HSO_4{}^-}$, $\mu_{SO_2,SO_2,HSO_4{}^-}$, $\mu_{SO_2,NH_4{}^+,SO_4{}^{2-}}$, $\mu_{SO_2,SO_4{}^{2-},SO_4{}^{2-}}$, and $\mu_{SO_2,SO_2,SO_4{}^{2-}}$ were all set to zero.

The experimental results for pressures above $\{SO_2 + (NH_4)_2SO_4 + H_2O\}$ [4] are shown in Fig. 4 $\{\bar{m}_{(NH_4)_2SO_4} \approx 2$ and $4\,\mathrm{mol\,kg^{-1}}\}$ in comparison with calculation results from the present correlation (full curves) as well as from the correlation by Rumpf and Maurer [4] (broken curves). The average absolute/relative deviation between experimental and correlated total pressures amount to ±0.014 MPa/2.3% (±0.018 MPa/2.4% for the correlation by Rumpf and Maurer). As expected, the new correlation does not yield a significant improvement when just the gas solubility is considered.

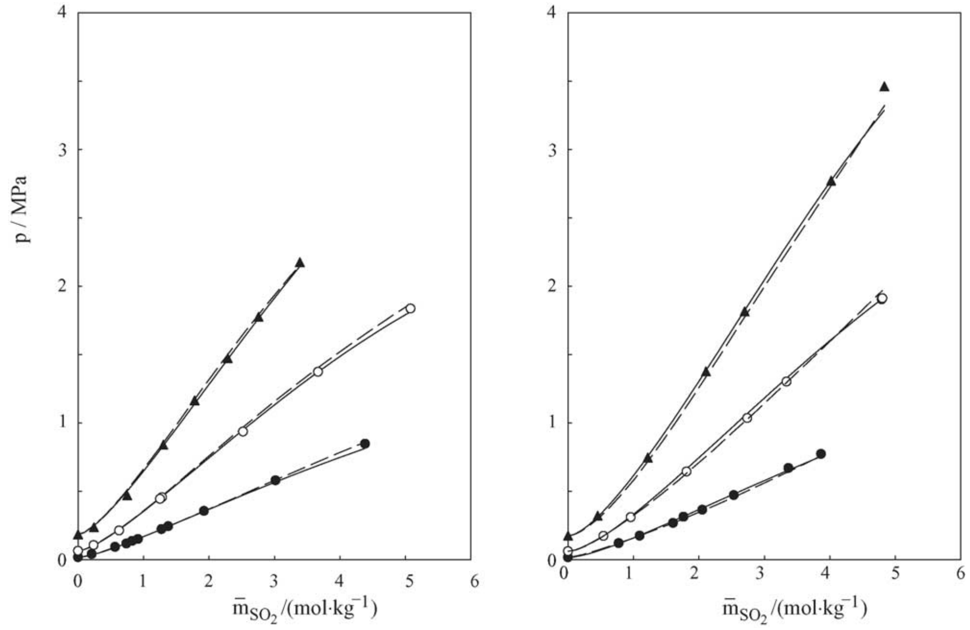

Fig. 4. Total pressure above solutions of $\{SO_2 + (NH_4)_2SO_4 + H_2O\}$, $\{\bar{m}_{(NH_4)_2SO_4} \approx 2\,\mathrm{mol\,kg^{-1}}$ in the left diagram, and $4\,\mathrm{mol\,kg^{-1}}$ in the right diagram$\}$: [(●) (333.15 K), (○) (363.15 K), (▲) (393.15 K)] experimental results from Rumpf and Maurer [4]; (—) correlation, this work; (– – –) correlation from Rumpf and Maurer [4].

Fig. 1 shows the correlation results (full curves) for the enthalpy change upon diluting liquid mixtures of $\{\mathrm{SO_2 + (NH_4)_2SO_4 + H_2O}\}$ in liquid mixtures of $\{\mathrm{(NH_4)_2SO_4 + H_2O}\}$ in comparison with experimental results. The correlation curves were calculated with averaged numerical values for the amounts of masses in the upper and the lower chamber and averaged numerical values for the stoichiometric salt molality. A detailed comparison (calculated from the exact experimental numbers for the amounts of those masses and the stoichiometric salt molality) is given in Table 1. The absolute deviation between the experimental results and the correlation results is in most cases within the estimated experimental uncertainty (cf. Table 1) and amounts in average to ±1.2 J. Furthermore, Fig. 1 shows predictions from the model by Rumpf and Maurer [4] (broken curves), where interaction parameters were solely fitted to the gas solubility data. That model results in an average absolute deviation between experimental and predicted enthalpy changes of ±32 J. That comparison demonstrates the improvement achieved by the extended model.

6.7. *($Na_2SO_4 + H_2O$) system*

The correlation equations for the three (temperature dependent) Pitzer parameters describing interactions between $\mathrm{Na^+}$ and $\mathrm{SO_4{}^{2-}}$ in aqueous solutions ($\beta^{(0)}_{\mathrm{Na^+,SO_4{}^{2-}}}$, $\beta^{(1)}_{\mathrm{Na^+,SO_4{}^{2-}}}$, and $C^{\phi}_{\mathrm{Na_2SO_4}}$) were adopted from Rogers and Pitzer [27]. ($\mu_{\mathrm{Na^+,Na^+,SO_4{}^{2-}}}$ was set equal to $\sqrt{2}/6C^{\phi}_{\mathrm{Na_2SO_4}}$, and $\mu_{\mathrm{Na^+,SO_4{}^{2-},SO_4{}^{2-}}}$ was set to zero.) The parameters are based on experimental information for the osmotic coefficient and from calorimetric investigations {for salt concentrations up to the solubility limit, which is about 3.4 (3.0) mol kg^{-1} at $T = 313$ K (353 K), cf., e.g., Seidell and Linke [28]} and can be used from about $T = 298$–473 K. Some more experimental investigations of that system as well as more precise correlations of its thermodynamic properties have been presented recently (after the publication of Rogers and Pitzer [27]), cf., e.g., Rumpf et al. [6] and Rard et al. [29]. But, as the experimental results reported by Rumpf et al. [6], which cover the salt concentration and temperature ranges of the present investigation, were perfectly predicted by applying the correlation of Rogers and Pitzer [27], there was no need to modify the G^{E}-equation presented here.

6.8. *($NaHSO_3 + H_2O$) or ($Na_2S_2O_5 + H_2O$) system*

Ermatchkov et al. [1] reported the results of experimental investigations (by IR-spectroscopy and batch-calorimetry) at temperatures between 313 and 353 K together with correlation equations for the (temperature dependent) Pitzer parameters describing interactions (in aqueous solutions) between $\mathrm{Na^+}$ and $\mathrm{HSO_3{}^-}$ ($\beta^{(0)}_{\mathrm{Na^+,HSO_3{}^-}}$, $\beta^{(1)}_{\mathrm{Na^+,HSO_3{}^-}}$, and $C^{\phi}_{\mathrm{NaHSO_3}}$) as well as between $\mathrm{Na^+}$ and $\mathrm{S_2O_5{}^{2-}}$ ($\beta^{(0)}_{\mathrm{Na^+,S_2O_5{}^{2-}}}$, $\beta^{(1)}_{\mathrm{Na^+,S_2O_5{}^{2-}}}$, and $C^{\phi}_{\mathrm{Na_2S_2O_5}}$). These Pitzer parameters were adopted here. Table 5 gives the correlation equations for $\beta^{(0)}_{\mathrm{Na^+,HSO_3{}^-}}$ and $\beta^{(0)}_{\mathrm{Na^+,S_2O_5{}^{2-}}}$. The parameters $\beta^{(1)}_{\mathrm{Na^+,HSO_3{}^-}}$, $C^{\phi}_{\mathrm{NaHSO_3}}$ (i.e., $\mu_{\mathrm{Na^+,Na^+,HSO_3{}^-}}$ and $\mu_{\mathrm{Na^+,HSO_3{}^-,HSO_3{}^-}}$), $\beta^{(1)}_{\mathrm{Na^+,S_2O_5{}^{2-}}}$, and $C^{\phi}_{\mathrm{Na_2S_2O_5}}$ (i.e., $\mu_{\mathrm{Na^+,Na^+,S_2O_5{}^{2-}}}$ and $\mu_{\mathrm{Na^+,S_2O_5{}^{2-},S_2O_5{}^{2-}}}$) are all set to zero.

6.9. *($SO_2 + NaHSO_3 + H_2O$) and ($SO_2 + Na_2S_2O_5 + H_2O$) systems*

There is no experimental (solubility and calorimetric) information for these systems available in the literature (which is probably due to their highly corrosive character). However, some of the Pitzer parameters describing interactions between $\mathrm{SO_2}$, $\mathrm{Na^+}$, and $\mathrm{HSO_3{}^-}$ and between $\mathrm{SO_2}$, $\mathrm{Na^+}$, and $\mathrm{S_2O_5{}^{2-}}$ (namely $\beta^{(0)}_{\mathrm{SO_2,HSO_3{}^-}}$, $\mu_{\mathrm{SO_2,HSO_3{}^-,HSO_3{}^-}}$, $\mu_{\mathrm{SO_2,SO_2,HSO_3{}^-}}$, $\beta^{(0)}_{\mathrm{SO_2,S_2O_5{}^{2-}}}$, $\mu_{\mathrm{SO_2,S_2O_5{}^{2-},S_2O_5{}^{2-}}}$, and $\mu_{\mathrm{SO_2,SO_2,S_2O_5{}^{2-}}}$) have already been used in previous sections. Due to the lack of experimental information, $\mu_{\mathrm{SO_2,Na^+,HSO_3{}^-}}$ and $\mu_{\mathrm{SO_2,Na^+,S_2O_5{}^{2-}}}$ had to be set to zero. The remaining parameters ($\beta^{(0)}_{\mathrm{SO_2,Na^+}}$, $\mu_{\mathrm{SO_2,Na^+,Na^+}}$, and $\mu_{\mathrm{SO_2,SO_2,Na^+}}$) are determined in the next section.

6.10. *($NaHSO_4 + H_2O$), ($SO_2 + Na_2SO_4 + H_2O$), ($SO_2 + NaHSO_4 + H_2O$) systems*

Pitzer's method requires the following (temperature dependent) parameters describing interactions in those aqueous solutions: (1) for interactions between $\mathrm{Na^+}$ and $\mathrm{HSO_4{}^-}$: $\beta^{(0)}_{\mathrm{Na^+,HSO_4{}^-}}$, $\beta^{(1)}_{\mathrm{Na^+,HSO_4{}^-}}$, and $C^{\phi}_{\mathrm{NaHSO_4}}$, (2) for interactions between $\mathrm{SO_2}$, $\mathrm{Na^+}$, and $\mathrm{SO_4{}^{2-}}$: $B^{(0)}_{\mathrm{SO_2,Na_2SO_4}}$, $\Gamma_{\mathrm{SO_2,Na_2SO_4,Na_2SO_4}}$, and $\Gamma_{\mathrm{SO_2,SO_2,Na_2SO_4}}$, and (3) for interactions between $\mathrm{SO_2}$, $\mathrm{Na^+}$, and $\mathrm{HSO_4{}^-}$: $B^{(0)}_{\mathrm{SO_2,NaHSO_4}}$, $\Gamma_{\mathrm{SO_2,NaHSO_4,NaHSO_4}}$, and $\Gamma_{\mathrm{SO_2,SO_2,NaHSO_4}}$. Again, instead of the comprehensive parameters, parameters $\beta^{(0)}_{ij}$, $\beta^{(1)}_{ij}$, and μ_{ijk} were considered. They were simultaneously fitted to the experimental results for the solubility of $\mathrm{SO_2}$ in $(\mathrm{Na_2SO_4 + H_2O})$ reported by Rumpf and Maurer [4] (for T ≈ 313–393 K) and to the experimental results for the heat of dilution from the present work (at $T \approx 313$ and 352 K). In an optimization procedure, the difference between experimental and calculated results for the total pressure as well as for the enthalpy of dilution was minimized. Four parameters ($\beta^{(0)}_{\mathrm{Na^+,HSO_4{}^-}}$, $\beta^{(1)}_{\mathrm{Na^+,HSO_4{}^-}}$, $\beta^{(0)}_{\mathrm{SO_2,Na^+}}$, and $\mu_{\mathrm{SO_2,Na^+,SO_4{}^{2-}}}$) proved sufficient to describe the experimental results almost within experimental uncertainty. These parameters are given in Table 5. $\mu_{\mathrm{Na^+,Na^+,HSO_4{}^-}}$, $\mu_{\mathrm{Na^+,HSO_4{}^-,HSO_4{}^-}}$, $\mu_{\mathrm{SO_2,Na^+,HSO_4{}^-}}$, $\mu_{\mathrm{SO_2,Na^+,Na^+}}$, and $\mu_{\mathrm{SO_2,SO_2,Na^+}}$ were all set to zero.

The experimental results for pressures above $(\mathrm{SO_2 + Na_2SO_4 + H_2O})$ [4] are shown in Fig. 5 ($\bar{m}_{\mathrm{Na_2SO_4}} \approx$ 0.5 and 1 mol kg^{-1}) in comparison with calculation results from the present correlation (full curves) as well as from

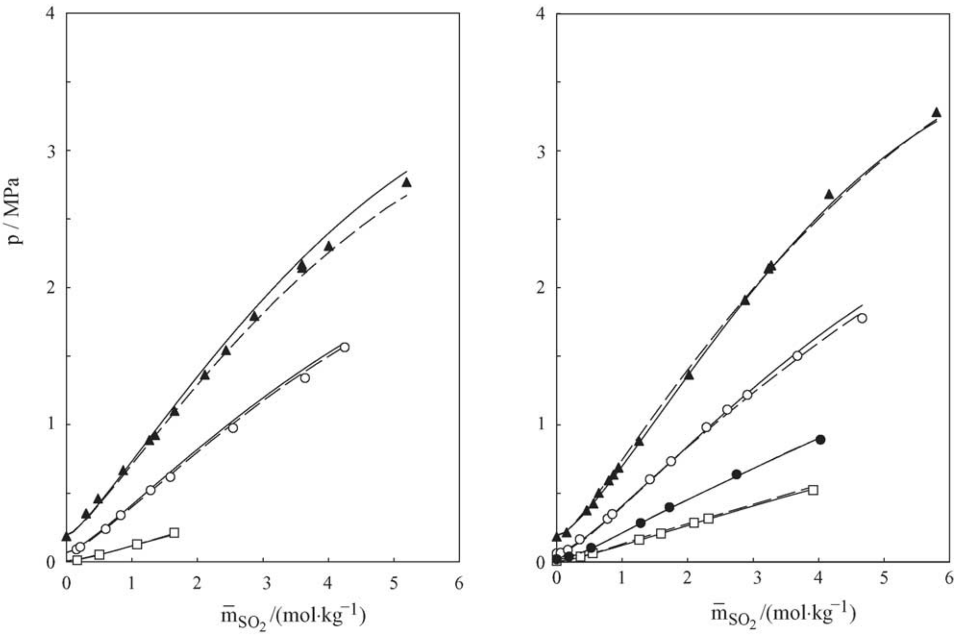

Fig. 5. Total pressure above solutions of ($SO_2 + Na_2SO_4 + H_2O$), ($\bar{m}_{Na_2SO_4} \approx 0.5$ mol kg^{-1} in the left diagram, and 1 mol kg^{-1} in the right diagram): [(□) (313.15 K), (●) (333.15 K), (○) (363.15 K), (▲) (393.15 K)] experimental results from Rumpf and Maurer [4]; (—) correlation, this work; (– – –) correlation from Rumpf and Maurer [4].

the correlation by Rumpf and Maurer [4] (broken curves). Both correlations are equally suited to describe the gas solubility data. The average absolute/relative deviation between experimental and correlated total pressures amount to ±0.024 MPa/3.4% (±0.020 MPa/3.2% for the correlation by Rumpf and Maurer).

Fig. 2 shows the correlation results (full curves) for the enthalpy change upon diluting liquid mixtures of ($SO_2 + Na_2SO_4 + H_2O$) in liquid mixtures of ($Na_2SO_4 + H_2O$) in comparison with experimental results. The correlation curves were calculated with averaged numerical values for the amounts of masses in the upper and the lower chamber and averaged numerical values for the stoichiometric salt molality. A detailed comparison (calculated from the exact experimental numbers for the amounts of those masses and the stoichiometric salt molality) is given in Table 2. The absolute deviation between the experimental results and the correlation results is in most cases within the estimated experimental uncertainty (cf. Table 2), and amounts in average to ±2.6 J. Furthermore, Fig. 2 shows predictions from the model by Rumpf and Maurer [4] (broken curves), where interaction parameters were solely fitted to the gas solubility data. The average absolute deviation between experimental and predicted enthalpy changes amounts to ±35 J. This comparison again demonstrates the improvement achieved by the new correlation.

7. Comparison with literature data

No experimental information on the enthalpy change neither upon diluting aqueous solutions of $\{SO_2 + (NH_4)_2SO_4\}$ by aqueous solutions of $(NH_4)_2SO_4$ nor upon diluting aqueous solutions of ($SO_2 + Na_2SO_4$) by aqueous solutions of Na_2SO_4 could be found in the open literature. In addition, except for the experimental data reported by Rumpf and Maurer [4], which were used to parameterize the model, literature data for the solubility of sulfur dioxide in aqueous solutions of ammonium or sodium sulfate are extremely scarce. Fox [30] investigated the solubility of sulfur dioxide in aqueous solutions of many different salts including ammonium and sodium sulfate (at $T = 298.15$ and 308.15 K), but these data could not be evaluated, because it is not possible to reliably convert the gas concentrations reported by Fox to molalities. The comparison with literature data is therefore restricted to the experimental data for the solubility of sulfur dioxide in aqueous solutions of sodium sulfate reported by Hudson [31] (23 data points at T ≈ 293–323 K, $\bar{m}_{Na_2SO_4}$ up to about 1.4 mol kg^{-1}, $\bar{m}_{SO_2}$ from about 0.7 to 1.7 mol kg^{-1}, and at a constant partial pressure of sulfur dioxide of 101.325 kPa). The average (maximum) relative deviation between the experimental data for the partial pressure of sulfur dioxide and the predictions from the new model amount to 2.8% (8.2%), 2.3% (3.4%), 1.8% (2.6%), and 1.4% (2.4%) at 293.15, 303.15, 313.15, and 323.15 K, respectively, which (except for one single data point) is well within the estimated experimental uncertainty. Applying the model by Rumpf and Maurer [4] those deviations amount to 16% (53%), 7.6% (39%), 7% (24.4%), and 5% (10.5%), respectively. Obviously, taking into account the formation of pyrosulfite and the new experimental information on the enthalpy change upon dilution results in much better predictions for the gas solubility.

8. Conclusions

New experimental results are presented for the enthalpy change upon diluting liquid mixtures of $(SO_2 + M_2SO_4 + H_2O)$ in liquid mixtures of $(M_2SO_4 + H_2O)$, where M = Na and NH_4, at about 313 and 352 K. A previously developed thermodynamic model (Rumpf and Maurer [4]) describing the vapor–liquid equilibrium of the chemical reacting systems $(SO_2 + M_2SO_4 + H_2O)$ is revised by additionally taking into account the results of the new calorimetric investigation. Although model predictions reveal that pyrosulfite may not appear in high concentrations in the aqueous solutions investigated in the present work, in contrary to the previous model, the formation of pyrosulfite is taken into account by the new model (cf. Ermatchkov et al. [1]), in order to enable a smooth transition to the quaternary systems $\{NH_3 + SO_2 + (NH_4)_2SO_4 + H_2O\}$ and $\{NH_3 + SO_2 + Na_2SO_4 + H_2O\}$, which will be investigated in a forthcoming publication. The previous model and the model presented here describe the gas solubility data of the systems $(SO_2 + M_2SO_4 + H_2O)$ reported by Rumpf and Maurer [4] with the same degree of accuracy. The new model additionally is able to accurately describe the results from the calorimetric investigations of these systems.

Acknowledgement

Financial support from DFG (Deutsche Forschungsgemeinschaft, grant PE 790/1-2) is gratefully acknowledged.

References

[1] V. Ermatchkov, Á. Pérez-Salado Kamps, G. Maurer, J. Chem. Thermodyn. 37 (2005) 187–199.

[2] U. Lichtfers, B. Rumpf, in: G. Maurer (Ed.): Thermodynamic Properties of Complex Fluid Mixtures, Research Report, Deutsche Forschungsgemeinschaft DFG, Wiley-VCH (ISBN 3-527-27770-6), 2004, pp. 92–119.

[3] U. Lichtfers, "Spektroskopische Untersuchungen zur Ermittlung von Speziesverteilungen im System Ammoniak-Kohlendioxid-Wasser", 2000. PhD Dissertation, University of Kaiserslautern, Germany.

[4] B. Rumpf, G. Maurer, Fluid Phase Equilib. 91 (1993) 113–131.

[5] Á. Pérez-Salado Kamps, E. Meyer, V. Ermatchkov, G. Maurer, "Enthalpy of dilution of $(SO_2 + H_2O)$ and of $(SO_2 + NH_3 + H_2O)$ in pure water: experimental results and modeling", Fluid Phase Equilib. (2005) (web-released: 23-Mar-2005).

[6] B. Rumpf, F. Weyrich, G. Maurer, Thermochim. Acta 303 (1997) 77–91.

[7] F. Weyrich, B. Rumpf, G. Maurer, Thermochim. Acta 359 (2000) 11–22.

[8] F. Weyrich, "Untersuchungen zum kalorischen Verhalten von Gemischen aus Ammoniak, Kohlendioxid, starken Elektrolyten und Wasser", 1997. PhD Dissertation, University of Kaiserslautern, Germany.

[9] H. Hasse, G. Maurer, Ber. Bunsen-Ges. Phys. Chem. 96 (1992) 83–96.

[10] R.N. Goldberg, V.B. Parker, J. Res. Natl. Bur. Stand. 90 (1985) 341–358.

[11] K.S. Pitzer, J. Phys. Chem. 77 (1973) 268–277.

[12] K.S. Pitzer, Activity Coefficients in Electrolyte Solutions, CRC, Boca Raton, 1991, p. 75.

[13] T.J. Edwards, G. Maurer, J. Newman, J.M. Prausnitz, AIChE J. 24 (1978) 966–976.

[14] K.S. Pitzer, R.N. Roy, L.F. Silvester, J. Am. Chem. Soc. 99 (1977) 4930–4936.

[15] B. Rumpf, G. Maurer, Fluid Phase Equilib. 81 (1992) 241–260.

[16] D.J. Bradley, K.S. Pitzer, J. Phys. Chem. 83 (1979) 1599–1603.

[17] A. Saul, W. Wagner, J. Phys. Chem. Ref. Data 16 (1987) 893–901.

[18] S.W. Brelvi, J.P. O'Connell, AIChE-J. 18 (1972) 1239–1243.

[19] Á. Pérez-Salado Kamps, Ind. Eng. Chem. Res. 44 (2005) 201–225.

[20] J.G. Hayden, J.P. O'Connell, Ind. Eng. Chem. Proc. Des. Dev. 14 (1975) 209–216.

[21] S. Pereda, K. Thomsen, P. Rasmussen, Chem. Eng. Sci. 55 (2000) 2663–2671.

[22] V.K. Filippov, M.V. Charykova, Yu.M. Trofimov, J. Appl. Chem. U.S.S.R. 58 (1985) 1961–1965.

[23] B. Rumpf, F. Weyrich, G. Maurer, Fluid Phase Equilib. 83 (1993) 253–260.

[24] H.F. Johnstone, Ind. Eng. Chem. 27 (1935) 587–593.

[25] H.F. Holmes, R.E. Mesmer, J. Chem. Thermodyn. 24 (1992) 317–328.

[26] S.L. Clegg, J.A. Rard, K.S. Pitzer, J. Chem. Soc. Faraday Trans. 90 (1994) 1875–1894.

[27] P.S.Z. Rogers, K.S. Pitzer, J. Phys. Chem. 85 (1981) 2886–2895.

[28] A. Seidell, W.W. Linke, Solubilities of Inorganic and Metal-Organic Compounds, vol. II, fourth ed., American Chemical Society, Washington, D.C., 1965.

[29] J.A. Rard, S.L. Clegg, D.A. Palmer, J. Solution Chem. 29 (2000) 1–49.

[30] C.J.J. Fox, Z. Phys. Chem. 41 (1902) 458–482.

[31] J.C. Hudson, J. Chem. Soc. 127 (1925) 1332–1347.